applied sciences

MDPI

Article

PIC Simulation of Enhanced Electron Acceleration in a Double Nozzle Gas Target Using Spatial–Temporal Coupling with Axiparabola Optics

Valdas Girdauskas [1,2], Vidmantas Tomkus [1], Mehdi Abedi-Varaki [1,*] and Gediminas Račiukaitis [1]

[1] Department of Laser Technologies, FTMC—Center for Physical Sciences and Technology, Savanoriu Ave. 231, 02300 Vilnius, Lithuania; valdas.girdauskas@ftmc.lt (V.G.); vidmantas.tomkus@ftmc.lt (V.T.); g.raciukaitis@ftmc.lt (G.R.)

[2] Department of Physics, Faculty of Natural Sciences, Vytautas Magnus University, K. Donelaicio St. 58, 44248 Kaunas, Lithuania

* Correspondence: m.abedi.varaki@gmail.com

Abstract: In this paper, the results of a Particle-in-Cell (PIC) simulation of electrons accelerated using a 10 fs Top-hat (TH) beam with a limited pulse energy of 85 mJ, focused on a double nozzle gas target using an off-axis parabola (OAP), an axiparabola (AXP), and an axiparabola with additional spatial–temporal coupling (AXP+STC), are discussed. The energy of accelerated electrons was predominantly determined through self-focusing and the ionisation injection effects of the laser beam propagating in plasma. The maximal energy of electrons accelerated using an AXP+STC could be higher by 12% compared to the energy of electrons accelerated by the regular OAP.

Keywords: laser wakefield acceleration; electron acceleration; top-hat laser beam; double nozzle gas target

Citation: Girdauskas, V.; Tomkus, V.; Abedi-Varaki, M.; Račiukaitis, G. PIC Simulation of Enhanced Electron Acceleration in a Double Nozzle Gas Target Using Spatial–Temporal Coupling with Axiparabola Optics. *Appl. Sci.* **2024**, *14*, 10611. https://doi.org/10.3390/app142210611

Academic Editors: Ephraim Suhir and Rongwei Fan

Received: 12 September 2024
Revised: 17 October 2024
Accepted: 15 November 2024
Published: 18 November 2024

1. Introduction

The laser wakefield acceleration (LWFA) of high-quality electron bunches is of high interest for several applications, such as the generation of secondary radiation, material science, imaging, or radiotherapy [1–4]. Very High Energy Electrons (VHEE) with energy >150 MeV and sufficient charge are required for the dose rate of the FLASH radiotherapy [5,6]. Emerging kHz-class lasers offer an attractive opportunity to develop reliable and stable VHEE sources; however, the pulse energy of kHz-class lasers is limited to approximately one hundred mJ [7]. One of the ways to increase the energy of accelerated electrons is to implement the focusing of the laser beam using new optic called an axiparabola (AXP), as reported by different research groups [8–10]. The AXP forms a Bessel-like laser beam with a prolonged focal area, extending the electron acceleration distance. In addition, applying spatio–temporal coupling (STC) could compensate for the dephasing of accelerating plasma waves [11]. In a recent paper, the LWFA simulation using an AXP to focus the laser pulse with the energy of 6.2 Joules demonstrated the feasibility of accelerating electrons over 20 dephasing lengths (1.3 cm) to a maximum energy of 2.1 GeV [12]. To ensure the required amount of accelerated charge, better control of ionisation injection, and the low energy dispersion of the VHEE source, a double nozzle with separate sections comprising a mixture of He and N_2 gases for injection and pure He for acceleration was proposed [13]. In this short note, three cases of a Particle-in-Cell (PIC) simulation of electrons, accelerated using a 10 fs Top-hat beam (TH) with a limited pulse energy of 85 mJ, and focused on a double nozzle target using an off-axis parabola (OAP), an axiparabola (AXP), and an axiparabola with spatial–temporal coupling (AXP+STC), are discussed.

2. Materials and Methods

Most high-intensity lasers generate beams with a TH, super-Gaussian energy distributor across the aperture. For the simulation of the LWFA of electrons using a TH laser beam, the quasi-3D Fourier–Bessel particle-in-cell (FBPIC) code version (0.25.0) was used [14]. The code employs the azimuthal modal decomposition method to describe the transverse profile of the laser beam, enabling the efficient simulation of the spatial–temporal evolution of the laser pulse in plasma with reduced computational resources. Three configuration cases were numerically investigated, using different approaches to focus the TH laser beam onto a gas target for laser wakefield acceleration:

- TH beam focused using an OAP;
- TH beam focused using an AXP;
- TH beam focused using an AXP+STC, allowing control of the laser pulse's front curvature.

In the simulations, a gas target consisting of two sections was used. The first section, which was L_n = 200 μm in length and with helium and a 1% nitrogen mixture, was implemented for the ionisation injection. The second section, which was 800 μm in length and with pure helium, was only used to accelerate electrons. Such a gas target could be manufactured from a single block of fused silica using 3D laser machining technology developed by FTMC located in Vilnius, Lithuania [15]. The configuration used in the PIC simulation is presented in Figure 1. The plasma density corresponding to the highest energy of accelerated electrons was $n_e = 1.2 \times 10^{19}$ cm^{-3}. In all the simulations, the total acceleration distance was 800 μm. The beginning of the plasma zone was at a distance of 25 μm, the ramp-up length of the plasma profile was 10 μm, and the peak of the laser pulse at the start of the simulation was a distance of 15 μm from z = 0 μm, i.e., in the middle of the flying coordinate window. The key parameters of the laser beams and plasma are provided in Table 1. Furthermore, the simulation inputs and associated computational details are included in Table 2. The TH transverse distribution of the intensity of the laser pulse incident to the OAP/AXP mirror with a Gaussian temporal envelope of the pulse was applied in the simulation. The Fresnel approximation was used to calculate the electric field of the laser wave at the focal plane.

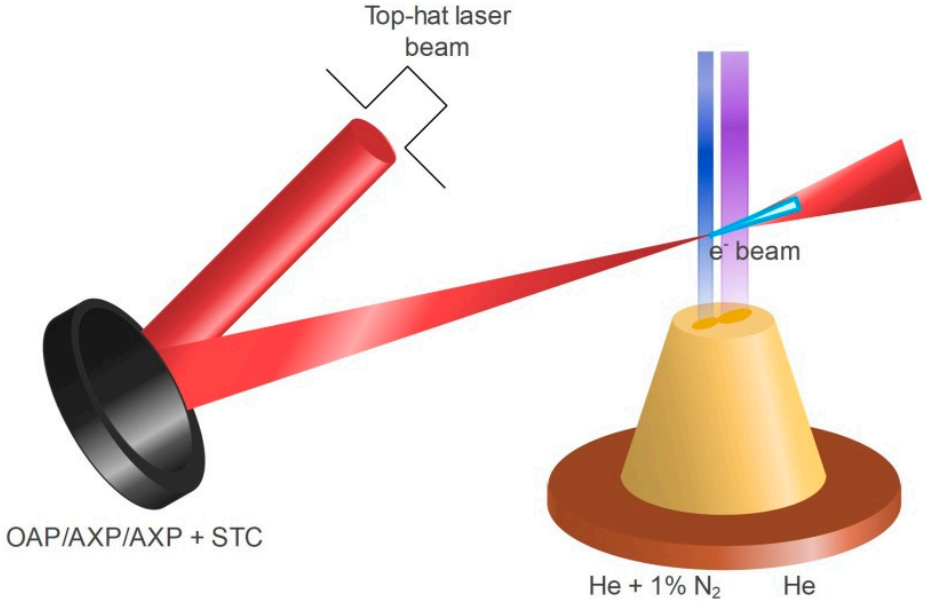

Figure 1. The simulation setup: A TH laser beam is focused using an OAP or AXP onto a double gas target with a section of the He+1%N_2 mixture used for electron injection and a pure He section for electron acceleration. The length of the gas jet section of the He mixture with 1% N_2 was L_n = 200 μm.

Table 1. Simulation parameters for laser and plasma.

Physical Parameters	Values
Pulse duration (FWHM), τ_0 (fs)	10
Pulse centre start position, z_0 (μm)	20
Pulse length (FWHM), $L_0 = c\tau_0$ (μm)	3
Laser strength parameter, a_0	1.5–2.5
Laser wavelength, λ (μm)	0.8
Laser pulse energy, (mJ)	85
Focus position, z_{foc} (μm)	430
Beam waist, w_0 (μm)	5
Rayleigh range for Gaussian beam, z_R (μm)	98
Rayleigh range for Bessel–Gauss beam, z_R (μm)	800
Hydrogen concentration, n_{atoms} (10^{19} cm^{-3})	1.2
Start position in z (μm)	0
Total z-extension, (μm)	800
Ramp length of the first nozzle (μm)	10
Ionisation injection zone length (μm)	200
Plasma wavelength, λ_p (μm)	9.5

Table 2. Computing parameters used in the FBPIC simulations.

Simulation Parameters	Values
Number of grid points along z	600
Number of grid points for Gaussian beam along r	300
Number of grid points for Bessel–Gauss beam along r	600
Number of particles per cell along z	2
Number of particles per cell along r	2
Number of particles per cell along θ	3
Number of azimuthal modes, n_m	3
Simulation box size along, z (μm)	30
Simulation box size for Gaussian beam along, r (μm)	60
Simulation box size for Bessel-Gaussian beam along, r (μm)	200
Speed of the moving window, $v_w(c)$	1
Simulation time step, Δt (fs)	1/3

For the simulation, an incident TH laser pulse with an energy of 85 mJ and a diameter of d = 50 mm was chosen. The focal lengths of the OAP and AXP were f = 400 mm, corresponding to the f/d = 8, the focal point z_f = 430 μm, and the focal depth of AXP δ = 800 μm. The longitudinal distributions of the peak-normalised vector potential (laser strength parameter) a_0 in the focal zone of the TH laser beam focused onto the vacuum using the OAP and the AXP used in the simulations are presented in Figure 2a. The simulations using an OAP were carried out for three cases: for the focal plane positions z_f = 30 μm, z_f = 330 μm, and z_f = 430 μm, starting the simulation at the plane z = 0 μm. This allowed us to evaluate the impact of initial starting values of laser strength parameter a_0 on the electron injection and acceleration process. The vertical dotted line indicates the length of the injection section of the gas target. The focal depth of AXP δ = 800 μm was chosen with the intention of maintaining the a_0 in the range of 1.5–2.5 for a laser pulse with an energy of 85 mJ. It results in a similar longitudinal a_0 profile of the beam, which was focused using both the OAP and AXP. In Figure 2b, the longitudinal distributions of the a_0 of the TH laser beam, which was focused on the vacuum for different values of the focal depth of the AXP δ = 0.8 mm, δ = 2.5 mm, and δ = 5 mm, are shown. The implementation of advantages of the long plateau of a_0, which is typical for the electron acceleration using an AXP to focus the pulse of the Joule class laser [9–11], is not relevant in the case of the limited pulse energy of kHz lasers The a_0 values drop below one for δ > 2.5 mm. For a small length of focal zone, the laser intensity is not constant along the focal zone of the AXP. It reaches its maximum value in the centre of the focal zone and drops down at the

edges. By reflecting the beam with the radial echelon, introducing a delay within the laser pulse depending on the radial coordinate, and focusing the laser beam with the AXP, it is possible to control the group velocity of the laser pulse in the focal zone of an AXP [11]. In this way, the spatial–temporal structuring of laser radiation allows us to compensate for the dephasing of the laser pulse in the plasma. When the pulse velocity in the plasma is equal to the speed of light in the vacuum, we have a dephasingless laser wakefield accelerator (DLWFA) mode when dephasing has a negligible effect on electron acceleration [16,17].

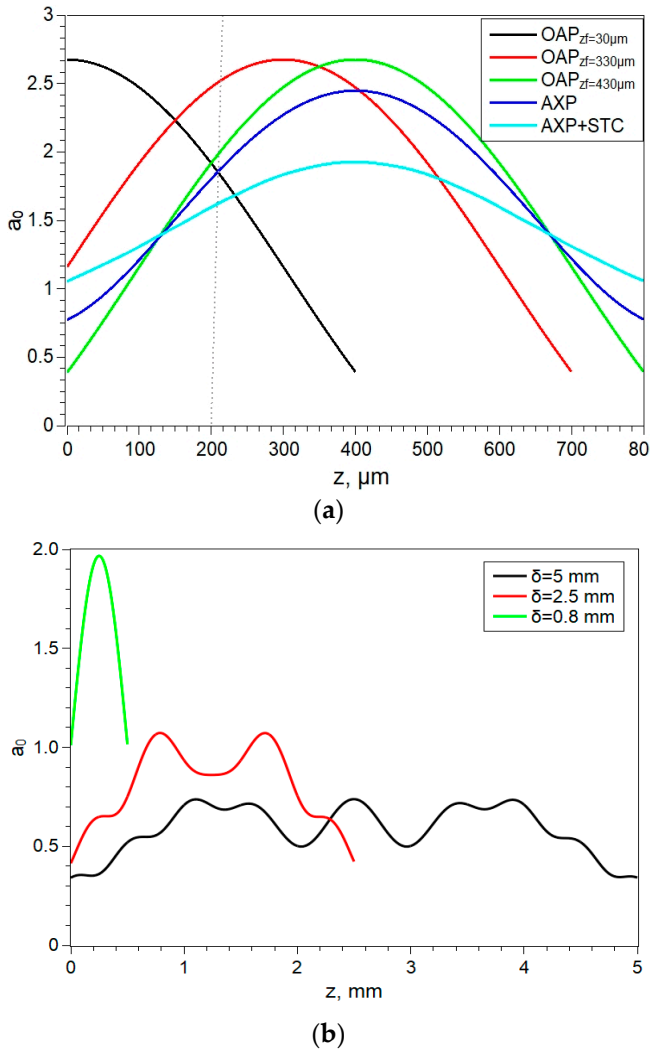

Figure 2. (**a**) The longitudinal distribution of the laser strength parameter a_0 in the vacuum at the focal zone of the 85 mJ TH laser beam, with the diameter d = 50 mm, which was focused using the OAP at the different points z_f = 30 μm, z_f = 330 μm, z_f = 430 μm, the AXP, and the AXP with STC α = 0.007. The vertical dotted line indicates the length of the injection section of the gas target. The focal lengths of the OAP and AXP are f = 400 mm, the focal point z_f = 430 μm, and the focal depth of AXP δ = 0.8 mm; (**b**) the longitudinal distribution of a_0 for different values of the focal depth of the AXP δ = 0.8 mm, δ = 2.5 mm, and δ = 5 mm.

To model the DLWFA mode, the temporal envelope of the laser pulse with the radial dependence of the pulse peak delay $E(r,t) = \exp\left(-\left(\left(t-\beta r^2\right)/\tau\right)^2\right)$ in the Fresnel integral was used to calculate the electric field at the focal plane, where the delay parameter $\beta = (\delta/c)\alpha$, and $\alpha = (v-c)/c$ defines the relative change in group velocity due to STC. The LWFA simulation of electrons using the AXP+STC was carried out for three cases of the STC parameter α = 0.005, α = 0.007, and α = 0.009. The simulation results

presented for the case of STC parameter α = 0.007 correspond to the highest energy of the accelerated electrons.

3. Discussions

The results of the LWFA simulation of electrons accelerated in plasma using the TH beam, focused using the OAP and the AXP+STC, are presented in Figures 3–5.

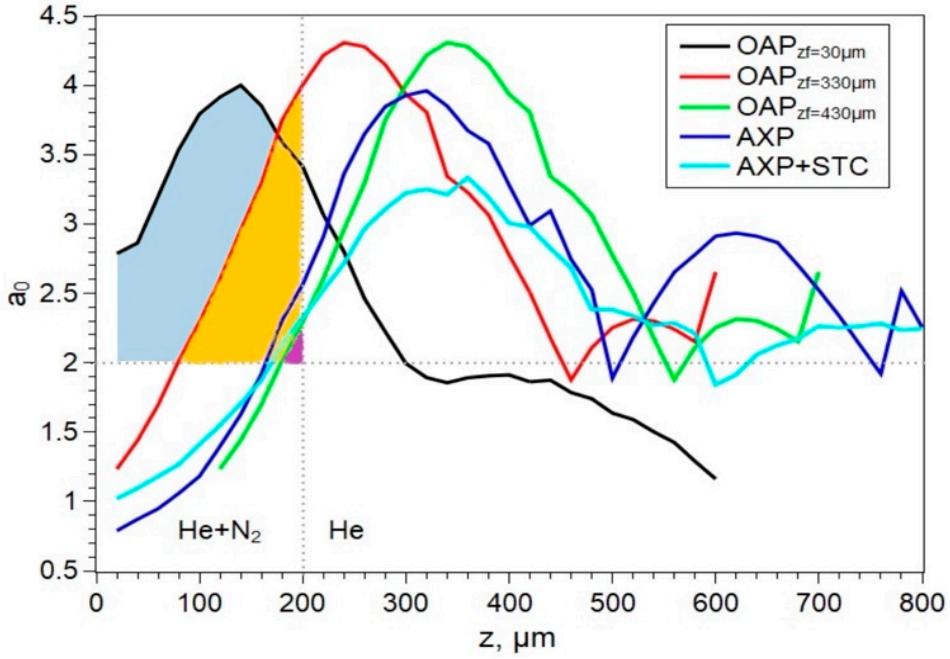

Figure 3. The dependence of the laser strength parameter a_0 of the TH laser pulse with an energy of 85 mJ, which was focused using an OAP towards the focal plane at z_f = 30 μm, z_f = 330 μm, and z_f = 430 μm, using an AXP with a focal zone length of 800 μm, and using an AXP with STC α = 0.007.

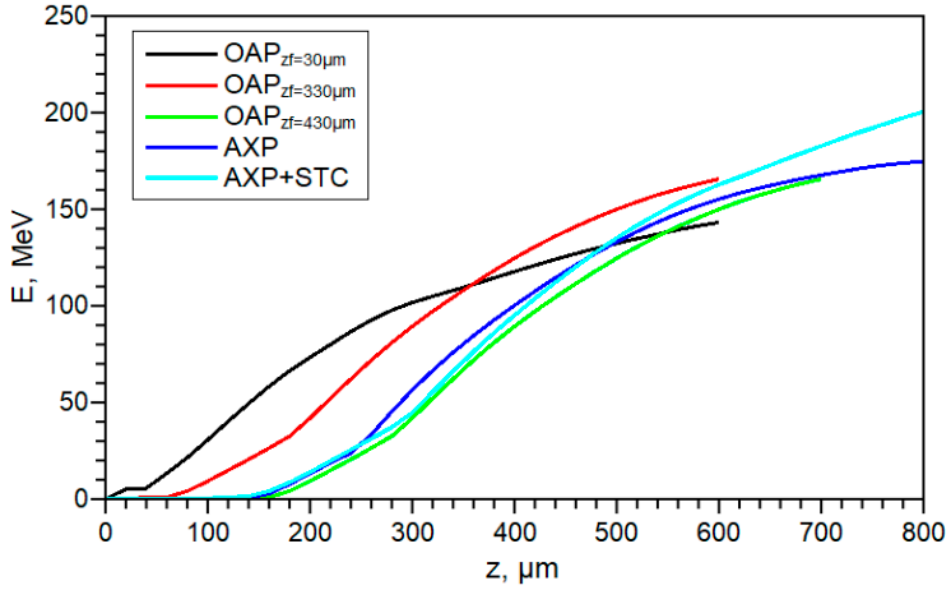

Figure 4. The maximal energy E_{max} of accelerated electrons using the TH laser pulse with an energy of 85 mJ, which was focused using the OAP towards the focal plane z_f = 30 μm, z_f = 330 μm and z_f = 430 μm, using the AXP, and using the AXP with STC α = 0.007. The plasma electron concentration was 1.2 × 10^{19} cm^{-3}, and the length of the ionisation injection zone in all cases was L_n = 200 μm.

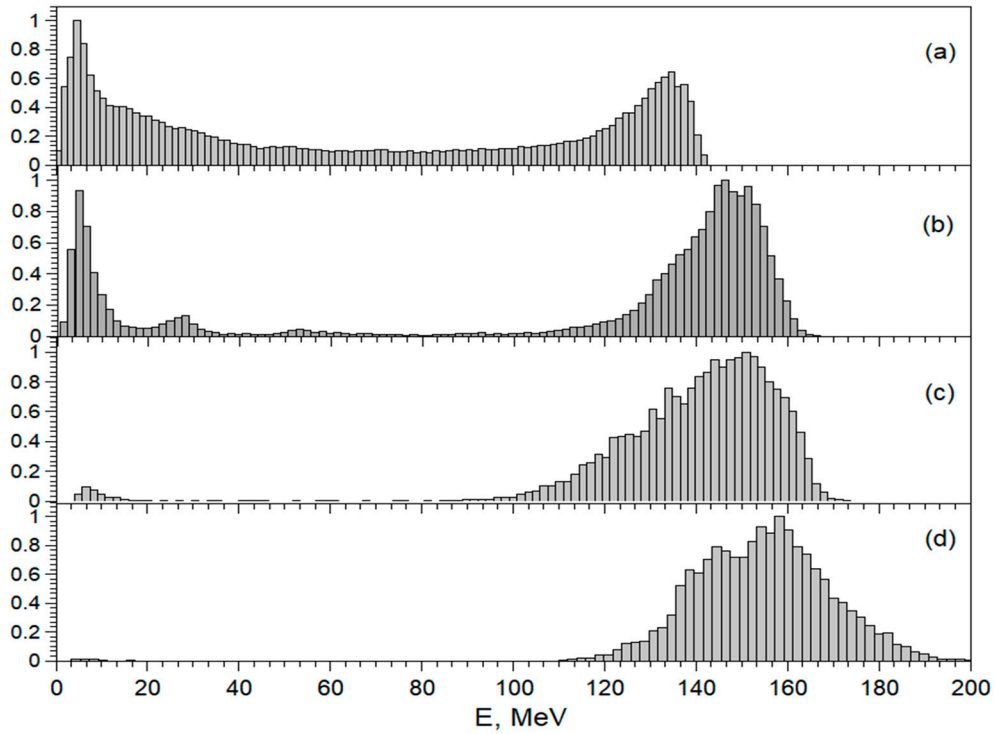

Figure 5. The energy spectra of accelerated electrons using the TH laser pulse with an energy of 85 mJ, which was focused using an OAP towards the focal planes z_f = 30 μm (**a**) and z_f = 330 μm. (**b**), using the AXP (**c**), and using the AXP with STC parameter α = 0.007 (**d**). The plasma electron concentration was 1.2 × 10^{19} cm^{-3}, and the total acceleration distance was 800 μm. The length of the ionisation injection zone in all cases was L_n = 200 μm.

The plasma electron concentration was 1.2 × 10^{19} cm^{-3}, and the length of the ionisation injection zone in all cases was L_n = 200 μm. The colour-marked areas represent the ionisation injection zone; area size correlates with the amount of accelerated charge and spread of the energy spectrum.

In Figure 3, the dependence of the laser strength parameter a_0 of the TH laser pulse, which was focused using an OAP towards the focal plane at z_f = 30 μm, z_f = 330 μm, and z_f = 430 μm, using the AXP, and using the AXP+STC with α = 0.007, propagating in a plasma medium with the electron concentration n_e = 1.2 × 10^{19} cm^{-3}, are presented. In all cases, the laser pulse undergoes self-focusing, and the peak of the laser strength parameter a_0 reaches a maximum value in the range of 3.3–4.4 in the focal zone. Despite the quite short Rayleigh length of z_R = 98 μm of the OAP, the distance where a_0 > 2 is approximately 500 μm long. In the case of the AXP, with a focal zone length of 800 μm, the distance where a_0 > 2 is slightly higher and extends over 700 μm. The initial starting values of the laser strength parameter a_0 affect the injection mechanism of electrons. The ionisation injection starts when a_0 > 2, and with a limited length of the ionisation injection zone L_n = 200 μm, the actual injection continues for as long as 200 μm for the OAP when focused onto the focal plane z_f = 30 μm, 100 μm when focused onto the focal plane z_f = 330 μm, and ~50 μm when focused onto the focal plane z_f = 430 μm, and when focused using the AXP. A shorter injection zone results in the formation of quasi-monoenergetic electron bunches, preferable for VHEE applications. However, the total charge of accelerated electrons becomes smaller. In such a way, adjusting the focal position inside the gas jet could help to control the ionisation injection length of electrons. The longitudinal distribution of the laser strength parameter a_0 in the focal zone of the focused TH laser beam for the AXP+STC case presented in Figure 3 is similar to the longitudinal distribution of the a_0 of the TH laser beam which was focused using the AXP. However, because of the longer dephasing length, the electrons reach higher energies (Figures 4 and 5). In Figure 4, the dependence of the maximal energy

E_{max} of the accelerated electrons on the acceleration distance is presented. The maximum energy E_{max} of the accelerated electron using the TH laser beam, which was focused using the OAP towards the focal plane z_f = 30 μm, reaches 130 MeV, and 170 MeV when focused towards the focal plane z_f = 330 μm. The maximum energy E_{max} of the accelerated electron using the TH laser beam which was focused using the AXP is 6% higher, and increases to 180 MeV. In the case of the AXP+STC, the maximal electron energy compared to the best OAP case increases by 12% and reaches 200 MeV.

In Figure 5, the energy spectra of accelerated electrons using the TH laser pulse, which was focused using the OAP towards the focal planes z_f = 30 μm (a) and z_f = 330 μm (b), using the AXP (c), and using the AXP with the STC parameter α = 0.007, are presented. The electron energy spectrum (Figure 5a) of the OAP focused on the focal plane z_f = 30 μm shows two peaks: one in the area of high energies, and the other in the area of low energies. The total charge of accelerated electrons is 30 pC. For the focal plane z_f = 330 μm, the share of low-energy electrons in the energy spectrum is lower (Figure 5b). However, the total charge of all electrons decreases to 12 pC. The average energy $E_{>0.8max}$ of electrons, in the interval from E_{max} to 0.8 E_{max}, is 100 MeV for z_f = 30 μm and 145 MeV for z_f = 330 μm. In the energy spectrum of accelerated electrons using the AXP, as shown in Figure 5c, some electrons of low energies are also visible. However, most of the accelerated electrons are concentrated in the high-energy part of the spectrum. When compared to the case where an OAP was used to focus the TH laser beam, the average energy $E_{>0.8max}$ increased to 150 MeV, and the total electron charge dropped to 3 pC.

The simulation results of electron acceleration using the AXP with STC are shown in Figure 5d. The average energy $E_{>0.8max}$ increased to 170 MeV, which is about 11% more than in the case of the AXP without STC. The total accelerated charge was 2.5 pC.

4. Conclusions

The results of the LWFA simulation of electrons using a 10 fs TH laser beam with a limited pulse energy of 85 mJ, which was focused using an OAP and an AXP+STC, have shown that the energy of accelerated electrons was predominantly determined by the self-focusing and ionisation injection effects of the laser beam propagating in plasma. The electrons accelerated using the OAP focused towards the focal plane z_f = 30 μm reached E_{max} = 130 MeV and 170 MeV when focused towards the focal plane z_f = 330 μm. The corresponding average energy $E_{>0.8max}$ of electrons, in the interval from E_{max} to 0.8 E_{max}, was 100 MeV and 145 MeV, respectively. The maximum energy E_{max} of the accelerated electron using the TH laser beam which was focused using the AXP was 6% higher—180 MeV, and, in the case of the AXP+STC, the maximal electron energy increased by 12% to 200 MeV, relative to the best OAP case. The corresponding average energy $E_{>0.8max}$ of electrons was 150 MeV and 170 MeV, respectively. We found that the process of the LWFA of electrons, using an OAP and AXP to focus the laser pulse with limited energy, is similar. An advantage to the energy gain and formation of a quasi-monoenergetic bunch is observed only in the AXP+STC case, and while choosing the appropriate distance of the injection zone. The initial starting values of the laser strength parameter a_0 affect the injection mechanism of electrons. The ionisation injection starts when $a_0 > 2$, and with a limited length of the ionisation injection zone L_n = 200 μm, the continuing injection within 200 μm for the OAP when focused onto the focal plane z_f = 30 μm forms two peaks in the electron spectra: one in the area of high energies, and the other in the area of low energies. The total charge of accelerated electrons is 30 pC. There is a shorter injection zone when the TH beam is focused using the OAP towards the focal plane of z_f = 330 μm, and using the AXP results in the formation of quasi-monoenergetic electron bunches. However, the total charge of accelerated electrons becomes smaller, down to 2.5–12 pC.

Author Contributions: V.G. conducted the physical analysis, established the methodology, performed the FBPIC simulation, and wrote the original draft. V.T. carried out the physical analysis and FBPIC simulation, and wrote the original draft. M.A.-V. performed the physical analysis and FBPIC simulation, and wrote the original draft. G.R. was responsible for defining the methodology, supervising the research, formulating the investigation's objectives, and revising and editing the manuscript. All authors have read and agreed to the published version of the manuscript.

Funding: The research leading to these results was funded by the Research Council of Lithuania under grant agreement No. S-MIP-21-3.

Institutional Review Board Statement: Not applicable.

Informed Consent Statement: Not applicable.

Data Availability Statement: The data that supports the findings of this study are available inside the paper.

Conflicts of Interest: The authors declare no conflict of interest.

Abbreviations

The following abbreviations are applied in this manuscript:

PIC	Particle-In-Cell
FBPIC	Fourier–Bessel Particle-In-Cell
TH	Top-Hat
OAP	Off-AxisParabola
AXP	AXiParabola
AXP+STC	AXiParabola with additional Spatial–Temporal Coupling
LWFA	Laser WakeField Acceleration
VHEE	Very High Energy Electrons
DLWFA	Dephasingless Laser WakeField Accelerator

References

1. Malka, V.; Faure, J.; Gauduel, Y.A.; Lefebvre, E.; Rousse, A.; Phuoc, K.T. Principles and applications of compact laser–plasma accelerators. *Nat. Phys.* **2008**, *4*, 447–453. [CrossRef]
2. Joshi, C.; Corde, S.; Mori, W. Perspectives on the generation of electron beams from plasma-based accelerators and their near and long term applications. *Phys. Plasmas* **2020**, *27*, 070602. [CrossRef]
3. Hooker, S.M. Developments in laser-driven plasma accelerators. *Nat. Photonics* **2013**, *7*, 775–782. [CrossRef]
4. Tomkus, V.; Girdauskas, V.; Abedi-Varaki, M.; Raciukaitis, G. Laser wakefield acceleration of electrons using Bessel–Gauss doughnut beams for accelerating beam guiding. *J. Plasma Phys.* **2023**, *89*, 905890209. [CrossRef]
5. DesRosiers, C.; Moskvin, V.; Bielajew, A.F.; Papiez, L. 150–250 MeV electron beams in radiation therapy. *Phys. Med. Biol.* **2000**, *45*, 1781. [CrossRef] [PubMed]
6. Ronga, M.G.; Cavallone, M.; Patriarca, A.; Leite, A.M.; Loap, P.; Favaudon, V.; Créhange, G.; De Marzi, L. Back to the future: Very high-energy electrons (VHEEs) and their potential application in radiation therapy. *Cancers* **2021**, *13*, 4942. [CrossRef] [PubMed]
7. Polanek, R.; Hafz, N.A.; Lécz, Z.; Papp, D.; Kamperidis, C.; Brunner, S.; Szabó, E.R.; Tőkés, T.; Hideghéty, K. 1 kHz laser accelerated electron beam feasible for radiotherapy uses: A PIC–Monte Carlo based study. *Nucl. Instrum. Methods Phys. Res. Sect. A Accel. Spectrometers Detect. Assoc. Equip.* **2021**, *987*, 164841. [CrossRef]
8. Smartsev, S.; Caizergues, C.; Oubrerie, K.; Gautier, J.; Goddet, J.-P.; Tafzi, A.; Phuoc, K.T.; Malka, V.; Thaury, C. Axiparabola: A long-focal-depth, high-resolution mirror for broadband high-intensity lasers. *Opt. Lett.* **2019**, *44*, 3414–3417. [CrossRef] [PubMed]
9. Oubrerie, K.; Andriyash, I.A.; Lahaye, R.; Smartsev, S.; Malka, V.; Thaury, C. Axiparabola: A new tool for high-intensity optics. *J. Opt.* **2022**, *24*, 045503. [CrossRef]
10. Geng, P.-F.; Chen, M.; Zhu, X.-Z.; Liu, W.-Y.; Sheng, Z.-M.; Zhang, J. Propagation of axiparabola-focused laser pulses in uniform plasmas. *Phys. Plasmas* **2022**, *29*, 112301. [CrossRef]
11. Liberman, A.; Lahaye, R.; Smartsev, S.; Tata, S.; Benracassa, S.; Golovanov, A.; Levine, E.; Thaury, C.; Malka, V. Use of spatiotemporal couplings and an axiparabola to control the velocity of peak intensity. *Opt. Lett.* **2024**, *49*, 814–817. [CrossRef] [PubMed]
12. Miller, K.G.; Pierce, J.R.; Ambat, M.V.; Shaw, J.L.; Weichman, K.; Mori, W.B.; Froula, D.H.; Palastro, J.P. Author Correction: Dephasingless laser wakefield acceleration in the bubble regime. *Sci. Rep.* **2024**, *14*, 4870. [CrossRef] [PubMed]
13. Golovin, G.; Chen, S.; Powers, N.; Liu, C.; Banerjee, S.; Zhang, J.; Zeng, M.; Sheng, Z.; Umstadter, D. Tunable monoenergetic electron beams from independently controllable laser-wakefield acceleration and injection. *Phys. Rev. Spec. Top.-Accel. Beams* **2015**, *18*, 011301. [CrossRef]

14. Lehe, R.; Kirchen, M.; Andriyash, I.A.; Godfrey, B.B.; Vay, J.-L. A spectral, quasi-cylindrical and dispersion-free Particle-In-Cell algorithm. *Comput. Phys. Commun.* **2016**, *203*, 66–82. [CrossRef]
15. Tomkus, V.; Mackevičiūtė, M.; Dudutis, J.; Girdauskas, V.; Abedi-Varaki, M.; Gečys, P.; Račiukaitis, G. Laser-machined two-stage nozzle optimised for laser wakefield acceleration. *J. Plasma Phys.* **2024**, *90*, 965900102. [CrossRef]
16. Palastro, J.; Shaw, J.; Franke, P.; Ramsey, D.; Simpson, T.; Froula, D. Dephasingless laser wakefield acceleration. *Phys. Rev. Lett.* **2020**, *124*, 134802. [CrossRef] [PubMed]
17. Caizergues, C.; Smartsev, S.; Malka, V.; Thaury, C. Phase-locked laser-wakefield electron acceleration. *Nat. Photonics* **2020**, *14*, 475–479. [CrossRef]